Defense Technical Information Center Compilation Part Notice

ADP011177

TITLE: Optimization of Active Control Systems for Suppressing Combustion Dynamics

DISTRIBUTION: Approved for public release, distribution unlimited

This paper is part of the following report:

TITLE: Active Control Technology for Enhanced Performance Operational Capabilities of Military Aircraft, Land Vehicles and Sea Vehicles [Technologies des systemes a commandes actives pour l'amelioration des performances operationnelles des aeronefs militaires, des vehicules terrestres et des vehicules maritimes]

To order the complete compilation report, use: ADA395700

The following component part numbers comprise the compilation report:
ADP011101 thru ADP011178

Optimization of Active Control Systems for Suppressing Combustion Dynamics

Kwanwoo Kim
Jongguen Lee
Jacob Stenzler
Domenic A. Santavicca

Department of Mechanical and Nuclear Engineering
132 Research Building East
The Pennsylvania State University
University Park, PA 16802, USA

Abstract

Results from an experimental study of active combustion control using modulated secondary fuel on a laboratory-scale, lean premixed dump combustor are presented. A simple phase-delay, closed-loop controller was used for these tests operating at the 4th sub-harmonic of the dominant frequency of the instability. Tests were conducted using both natural gas and Jet-A as the secondary fuel and the results are compared. Of particular interest are the observed differences in control effectiveness and the causes of those differences.

Introduction

Suppression of combustion dynamics in gas turbine combustors using active combustion control with fuel flow modulation has been successfully demonstrated [1-16] in a number of laboratory-scale combustors and at least one full-scale combustor. Both modulated primary fuel injection and modulated secondary fuel injection have been employed in these demonstrations, as has sub-harmonic injection and both open-loop and closed-loop control. Among these successful demonstrations, however, significant variations in control effectiveness have been observed, not to mention the unreported cases where poor or no control was achieved. An important question is, can the results of these tests be used to make a meaningful assessment of the full potential of active combustion control? The answer to this question is no, and the reason is that in most of these tests the active control system was not optimized for maximum control effectiveness. This in turn raises another question, which is, how does one optimize an active combustion control system. In the case of modulated secondary fuel flow the main technical goal is to achieve (nearly) complete suppression of the pressure oscillations with minimum secondary fuel flow. Minimum secondary fuel is necessary in order to reduce the NO_x penalty that typically results from secondary fuel injection and to minimize the demands on the injector. There are a number of parameters which determine the effectiveness of a control system employing secondary fuel injection, including the phase, duration and frequency of injection, the injection pressure and the number and location of secondary injection sites. What these parameters have in common is that they all provide a means for changing the spatial and temporal fuel distribution in the combustor. Therefore it is reasonable to argue that optimization of an active combustion control system employing modulated secondary fuel injection can be viewed in a more general sense as optimization of the temporal and spatial distribution of the secondary fuel. One of the numerous factors affecting the secondary fuel distribution is whether the secondary fuel is gas or liquid. In this paper preliminary results are presented from a study of active combustion control of a lean premixed combustor employing modulated secondary fuel injection where a comparison is made of the control effectiveness that is achieved using natural gas and Jet-A as the secondary fuel.

Description of Experiment

Combustor

The coaxial dump combustor used in this study is illustrated schematically in Figure 1. The combustor consists of a mixing section and a

Paper presented at the RTO AVT Symposium on "Active Control Technology for Enhanced Performance Operational Capabilities of Military Aircraft, Land Vehicles and Sea Vehicles", held in Braunschweig, Germany, 8-11 May 2000, and published in RTO MP-051.

combustor section, separated by a dump plane. At the inlet of the 36 mm diameter by 330 mm long mixing section the flow is choked. The flame is stabilized on a bluff centerbody which is mounted flush with the dump plane. The 19 mm diameter centerbody is centered in the mixing section using vanes positioned at an angle of 30°, which also serve as an axial swirler. The upstream end of the combustor section is made from a 110 mm diameter fused-silica cylinder and the downstream end is fabricated from a 80 mm diameter stainless steel tube. The overall combustor length is 875 mm, which corresponds to a nominal L/D of 10. In these tests the combustor exit was partially-restricted ($A_{combustor}/A_{exit}$ = 17) but not choked. The primary fuel is natural gas (96% methane), which is introduced well upstream of the choked mixing section inlet, thus giving a uniform, premixed fuel-air distribution at the combustor entrance. In addition, because the fuel and air are mixed upstream of the choked inlet there is no possibility of feed-system coupling .

Measurements

Pressure oscillations are measured using water-cooled piezoelectric pressure transducers located in the dump plane, at various axial locations in the combustor (i.e., 1/2L, 3/4L and L) and in the mixing section. A photomultiplier tube (PMT) is used to monitor temporal variations in the chemiluminescence intensity from the flame. Although there is no general, quantitative correlation between the intensity of flame luminosity and other physical quantities, the chemiluminescence from various flame-radicals such as OH*, C_2*, CH* and CO_2* has been used as an indicator of both global and local heat release in lean premixed hydrocarbon flames [17-20]. In this study, a broad band-pass filter (BG-40) is used to collect the chemi-luminescence from CO_2* which is assumed to provide a qualitative measure of the flame's heat release.

In addition to the PMT chemilumine-scence measurements, an intensified CCD camera is used to record chemiluminescence images of the flame zone with a nominal 100mm by 150mm field of view. The measurements are phase-synchronized with the dump plane pressure measurement, giving a sequence of images which show the temporal and spatial evolution of the heat release distribution during one period of the pressure oscillation. A tomographic deconvolution procedure is used to extract the two-dimension heat release distribution from the original line-of-sight images [21].

And lastly, planar laser induced fluorescence is used to measure the fuel distribution at the annular exit of the mixing section.

Active Control System

An active control strategy based on the use of secondary fuel injection has been implemented using closed-loop control with 4th sub-harmonic injection and a simple phase-delay controller. The pressure transducer mounted in the dump plane is used as the sensor for the control system. The filtered output of the pressure transducer is fed into a custom-built control circuit where the threshold pressure level required to activate the secondary fuel injection valve is selected. The control circuit is also used to set the phase-delay between the pressure signal and the TTL input to the secondary fuel injection valve driver (General Valve Co., Iota One). Actuation, i.e., injection of secondary fuel, is initiated using a fast-acting solenoid valve (General Valve Co., Series 9). Note, that the fuel also flows through a manifold which delivers the fuel from the solenoid valve to the actual injectors.

As shown in Figure 2, secondary fuel is injected transversely into the mixing section through four air-assist injectors equally spaced around the circumference of the mixing tube and located 115mm upstream of the dump plane. Results with secondary injection of both natural gas and Jet-A fuel are presented. In the case of natural gas, no air-assist was used, while in the case of Jet-A the amount of air-assist was varied to investigate the effect of the spray characteristics on control effectiveness.

Results and Discussion

All of the results presented in this paper are for a combustor inlet temperature of 350°C, a combustor mean velocity of 5.25 m/s, and a nominal combustor pressure of 1.2 bar (~17.5 psia). As noted previously, the primary fuel is natural gas which is mixed with the air well upstream of the choked inlet to the mixing section, therefore the fuel distribution at the combustor inlet is uniform and there is no possibility of feed-system coupling. The stability map at this operating condition is shown in Figure 3, where the stability map is a plot of the rms pressure fluctuation in dB (measured by the pressure transducer mounted in the dump plane) versus the overall primary fuel-air equivalence

ratio. As shown in Figure 3, there is a 30 dB increase in the rms pressure fluctuation in going from the stable operating condition at an equivalence ratio of 0.65 to the unstable operating condition at an equivalence ratio of 0.55. For all of the active control results presented in this paper the combustor was operated at an equivalence ratio of 0.55, which is where the strongest instability occurs. The frequency spectrum of the pressure fluctuation at this condition shows that the dominant frequency is 336 Hz which corresponds to the first longitudinal mode of the combustor.

A sequence of twelve phase-synchronized chemiluminescence images, recorded in 30 degree phase angle increments, is shown in Figure 4 for the 0.55 equivalence ratio operating condition. (Each image shown in Figure 4 is an ensemble average of 20 individual images.) These images show clear evidence that flame-vortex interaction plays an important role in the observed instability. Also shown in Figure 4 is the pressure oscillation at this condition, where the numbers on the pressure signal correspond to the numbers on the images. As expected the most intense image (#10) coincides closely with the maximum in the pressure fluctuation.

The first active control tests were run using natural gas as the secondary fuel. As mentioned previously 4th sub-harmonic injection was used in these tests. The results are shown in Figure 5 which is a plot of the reduction in the rms pressure fluctuation in dB versus the phase delay between the negative-going zero-crossing of the pressure oscillation and the leading edge of the trigger signal to the solenoid valve driver. The fuel supply pressure, measured upstream of the solenoid valve, was 150 psig and the time averaged secondary fuel flow rate was measured with a flow meter located upstream of the solenoid valve. The amount of secondary fuel was varied by varying the injection pulse width. Shown are results for three different injection pulse widths, i.e., three different secondary fuel flow rates. At a secondary fuel flow rate equal to 5.7% of the primary fuel flow rate, there is a small reduction in the rms pressure fluctuation, i.e., from 0 dB at a delay of about 1.2 msec to 5 dB at a delay of about 2.6 msec. In the second case, when the secondary fuel flow rate is increased to 6.8% of the primary fuel flow rate, a very pronounced phase dependence is observed for delays between about 2.3 msec and 3 msec, with a maximum reduction of 25 dB at a phase delay of about 2.4 msec. When the secondary fuel flow rate is increased to 7.8% of the primary fuel flow rate, the strong phase dependence is somewhat diminished and effective control, i.e., dB reductions from 20 dB to 30 dB, are observed over the entire range of delay times.

In an attempt to explain these observations, measurements were made of the flame response function. The flame response function is the heat release as a function of time and space due to the injected secondary fuel and it is measured under stable flame conditions. Using the PMT to detect the total CO_2* chemiluminescence as a function of time provides an indication of the temporal variation in the heat release due to the injected secondary fuel. Such measurements are shown in Figure 6 for a range of injection pulse widths. The arrow in this figure shows the leading edge of the trigger signal to the solenoid valve driver, which occurs approximately every 11 msec. There is a delay of about 5 msec. between the solenoid valve trigger signal and the onset of the heat released by the secondary fuel pulse, which is primarily due to the convection time from the point of secondary fuel injection to the flame front. The half-height width of the flame response function shown in Figure 6 is approximately 5 msec, which is about twice the nominal 2.8 msec period of the pressure oscillation. Under these conditions it is somewhat surprising that the control effectiveness depends on the phase of the secondary injection as shown in Figure 5. Apparently the reason for this is the fact that the rise-time of the flame response function is only about 1 msec, which is a fraction of the period of the pressure oscillation.

Next, the results obtained using Jet-A for the secondary fuel are presented. The secondary fuel supply pressure, measured upstream of the solenoid valve, was 60 psig in these tests and the time averaged secondary fuel flow rate was measured with a flow meter located upstream of the solenoid valve. In these tests the time averaged secondary fuel flow rate was held constant at a value which corresponded to 8.6% of the heat release rate of the primary fuel flow. This corresponds to an injection pulse duration of 300 μsec. What was varied was the amount of air assist, which was varied by changing the pressure of the air assist supply line. Shown in Figure 7 is a plot of the reduction in the rms pressure fluctuation in dB versus the phase delay between the pressure oscillation and the trigger signal to the solenoid valve driver. Results are presented for the case with no air assist and for three different air assist pressures, i.e., 10, 15 and 25 psig. The first observation is that there is very

little phase dependence when Jet-A is used for the secondary fuel, although an effect on the magnitude of the rms pressure oscillations is observed. In the case with no air assist, the rms pressure oscillations actually increase by about 2 dB. With the air assist turned on at a pressure of 10 psig there is a 15 to 20 dB reduction in the rms pressure oscillations. However when the air assist pressure is further increased the control effectiveness is substantially diminished such that at an air assist pressure of 25 psig the reduction in the rms of the pressure oscillations is only about 5 dB. The results therefore indicate that there is an optimum air assist pressure in terms of achieving the greatest control.

Again the flame response function was measured in an attempt to explain the Jet-A results presented in Figure 7. In addition, PLIF measurements of the fuel distribution at the entrance to the combustor were also made for each of the air assist cases.

The temporal flame response function for the no air assist, 10 psig air assist and 25 psig air assist cases are shown in Figure 8. Compared to the natural gas case (Figure 6) the delay between the trigger signal and the onset of the secondary heat release has increased from about 5 msec. to about 8 msec. Similarly the rise-time of the heat release pulse has increased from about 1 msec in the natural gas case to about 2 msec in the 25 psig air assist case and about 3 msec in the 10 psig air assist and the no air assist cases. One possible explanation for this behavior is wall wetting due to liquid fuel impinging on the walls of the mixing section. The fact that with Jet-A the rise time has become comparable to the period of the pressure oscillation is possibly the reason why no phase dependence is observed in the Jet-A results. Additional insight into the fuel-air mixing process can be obtained from the fuel distribution measurements which are plotted in Figure 9. Shown are the fluorescence intensity profiles across the 8.5 mm wide annular opening between the outer wall of the centerbody and the inner wall of the mixer tube. Results are shown for all three air assist cases at 9 msec after the trigger signal. Under the conditions of these tests the measured intensities are linearly proportional to the fuel concentration, therefore meaningful comparisons between the results can be made. In the case with no air assist, the fuel concentration is noticeably less than in the other two cases and it increases by about a factor of two from the inner to outer wall of the mixing section. In the case with 25 psig air assist, the fuel concentration is significantly greater than in the no air assist case and increases from the outer to inner wall of the mixing section by about a factor of two. In the case with 10 psig air assist, the fuel concentration is about 50% greater than in the 25 psig air assist case and about 3 times greater than in the no air assist case. The fuel concentration profile is greatest at both the inner and outer walls of the mixing section, with a minimum in between.

The obvious question is can these results explain why the case with 10 psig air assist is so much more effective at controlling the instability. One possible explanation is as follows. In the no air assist case the results in Figures 8 and 9 suggest that the liquid fuel enters the mixing section but then is immediately diverted along the outer wall of the mixing section. Because the liquid fuel wets the outer wall, the rate of fuel-air mixing is limited by the rate of evaporation and as a result the 300 μsec fuel pulse is effective spread out over the entire 11 msec between injections. This significantly diminishes the impact of the injected fuel.

In the 25 psig case, the results suggest that the air assist is effectively transporting the liquid fuel across the annulus towards the inner wall of the mixing section. There is no evidence of significant wall wetting because the flame response function is relatively narrow in this case, but apparently having the secondary fuel along the inner wall of the mixing section is not very effective at controlling the instability.

In the 10 psig air assist case, the resultant fuel distribution seems to be an optimum compromise between the two other cases. The air assist appears to be sufficient to avoid the wall wetting that occurred in the no air assist case, yet not so strong as to transport most of the fuel across the annulus to the inner wall of the mixing section.

This interpretation is supported by a Rayleigh index analysis of the chemiluminescence images of the unstable flame presented in Figure 4. The Rayleigh index is the correlation between the local heat release fluctuations and the pressure fluctuations and identifies locations in the combustor where the instability is being most strongly driven. The Rayleigh index distribution for the instability depicted in Figure 4 is shown in Figure 10. The region of maximum positive Rayleigh index is the white region in the outer portion of the dump plane recirculation zone. If one were to argue that the secondary fuel needs to reach this location, then it seems reasonable that the 10 psig air assist case would be most effective at controlling the instability.

Conclusions

Active combustion control of combustion dynamics in a lean premixed dump combustor using modulated secondary fuel was studied using both natural gas and Jet-A as the secondary fuel. A simple phase delay controller and 4^{th} subharmonic injection was used for all of the tests. The results showed significant differences in control effectiveness when using Jet-A as compared to natural gas. With natural gas a relatively strong dependence on the phase delay between the pressure oscillation and the injection of secondary fuel was observed, whereas with Jet-A the control effectiveness was relatively insensitive to the phase delay. In the Jet-A tests an air assist injector was used which provided the capability of varying the spray characteristics by varying the air assist pressure. In these tests it was found that there was an optimum air assist pressure for which the greatest control was achieved. The differences between gas and liquid injection and the effects of air assist pressure could both be explained in terms of the spatial and temporal fuel distribution of the secondary fuel. In particular it was argued that differences in fuel penetration and the possibility of wall wetting with the liquid fuel were the main controlling factors.

Acknowledgements

This research was supported by the Office of Naval Research, under Grant #ND0014-96-1-0405, and is monitored by Dr. Gabriel D. Roy.

References

1. Candel, S.M., *Twenty-fourth Symposium (International) on Combustion,* The Combustion Institute, 1992, pp. 1277-1296.
2. Schadow, K.C. and Gutmark, E., *Prog. Energy Combust. Sci.*, Vol. 18, 1992, pp. 117-132.
3. McManus, K.R., Poinsot, T. and Candel, S.M., *Prog. Energy Combust. Sci.*,Vol. 19, 1993, pp. 1-29.
4. Poinsot, T., Bourienne, F., Candel, S., Esposito, E. and Lang, W., *J.* Propulsion, Vol. 5, No.1, 1989, pp.14-20.
5. Langhorne, P.J.,Dowling, A.P. and Hooper, N., *J.* Propulsion, Vol. 6, No. 3, 1990, pp.324-333.
6. Gulati, A. and Mani, R., *J. of Propulsion and Power,* Vol. 8, No. 5, 1992, pp. 1109-1115.
7. Billoud, G., Galland, M.A., Huu, C.H. and Candel, S., *Combust. Sci. and Tech.,* Vol. 81, 1992, pp.257-283.
8. Wilson, K.J., Gutmark, E., Schadow, K.C. and Smith, R.A., *J. of Propulsion and Power,* Vol.11, No. 2, 1995, pp. 268-274.
9. Sivasegaram, S., Tsai, R.F. and Whitelaw, J.H, *Combust. Sci. and Tech.,* Vol. 105, 1995, pp.67-83.
10. Richards, G.A., Yip, M.J., Robey, E., Cowell, L. and Rawlins, D., *J. of Engineering for Gas Turbines and Power,* Vol. 119, 1997, pp. 340-343.
11. Neumeier, Y. and Zinn, B.T., *Twenty-sixth Symposium (International) on Combustion,* The Combustion Institute, 1996, pp. 2811-2818.
12. Yu, K.H, Wilson, K.J. and Schadow, K.C., *Twenty-seventh Symposium (International) on Combustion,* The Combustion Institute, 1998, pp. 2039-2046.
13. Paschereit, C.O., Gutmark, E. and Weisenstein, W., *Combust. Sci. and Tech.,* Vol. 138, 1998, pp.213-232.
14. Jones, C.M., Lee, J.G. and Santavicca, D.A., *J. of Propulsion and Power,* Vol.15, No. 4, 1999, pp. 584-590.
15. Seume, J.R., Vortmeyer, N., Krause, W., Hermann, J., Hantschk, C.-C., Zangl, P., Gleis, S., Vortmeyer, D., Orthmann, A., ASME Paper# 97-AA-119, ASME ASIA '97 Congress & Exhibition, Singapore, Sept. 30-Oct.2, 1997.
16. Cohen, J.M., Rey, N.M., Jacobson, C.A. and Anderson, T.J., International Gas Turbine & Aeroengine Congress & Exhibition, Stockholm, Sweden, June 2-5, 1998.
17 Dandy, D.S. and Vosen, S.R., *Combust. Sci. and Tech.,* Vol. 82, 1992, pp.131-150.
18. Samaniego, J.-M, Egolfopoulos, F.N. and Bowman, C.T., *Combust. Sci. and Tech.,* Vol. 109, 1995, pp.183-203.
19. Najm, H.N., Paul P.H., Mueller, C.J. and Wyckoff, P.S., *Combustion and Flame,* Vol. 113, 1998, pp.312-332.
20. Bandaru, R.V., Miller, S., Lee, J.G. and Santavicca, D.A., Proceedings of SPIE- The International Symposium on Industrial and Environmental Monitors and Biosensors, Vol. 3535, pp. 104-114, Boston, MA, Nov. 2-5, 1998.
21. Dasch, C.J., *Applied Optics*, 31(6), 1992.

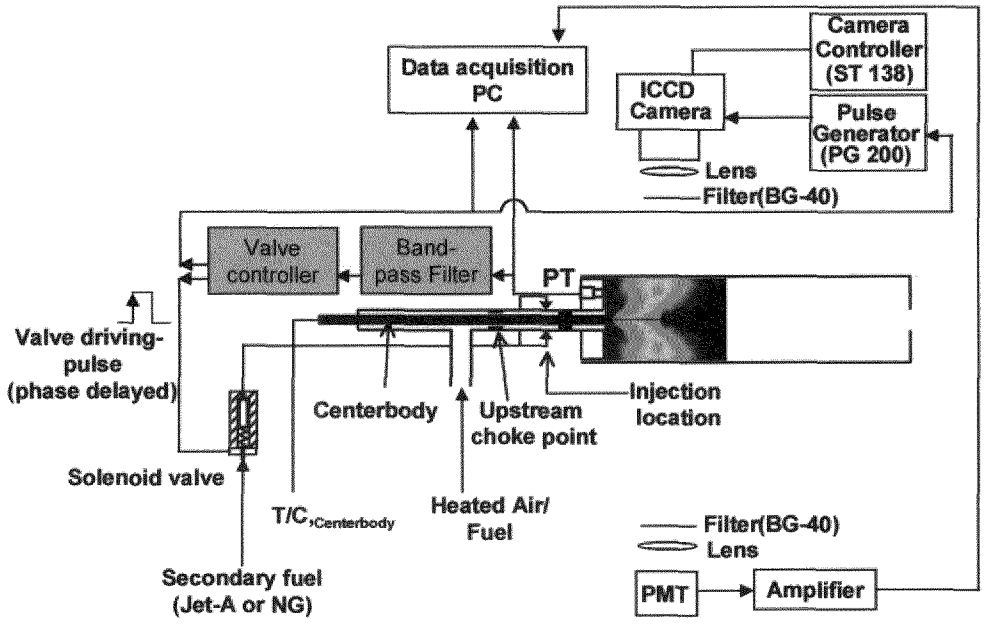

Figure 1. Experimental setup for active control and diagnostics

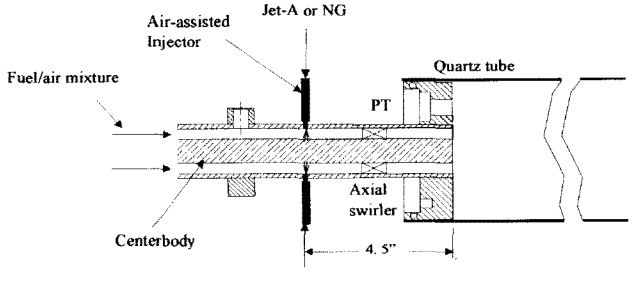

Figure 2. Schematic of mixer section of combustor and secondary fuel injection locations

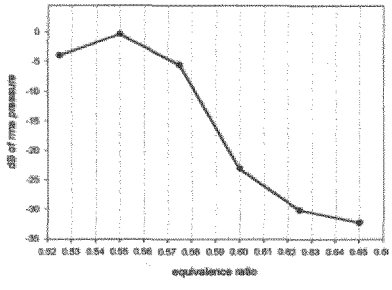

Figure 3. Stability map of the combustor (V=5.25m/sec, T_{in}=350°C)

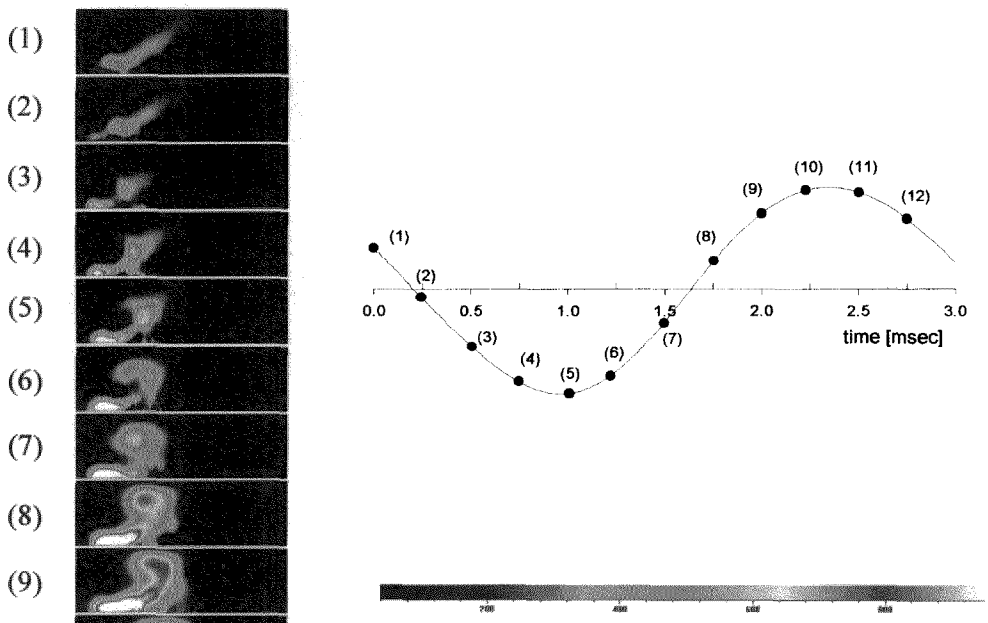

Figure 4. Phase-synchronized unstable flame images of CO_2* chemiluminescence
Φ=0.55, V=5.25m/sec, T_{in}=350°C, 100%PM

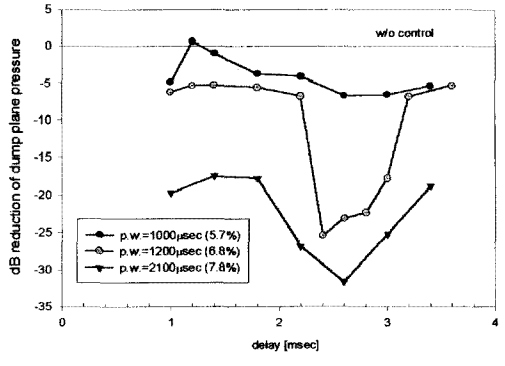

Figure 5. Phase dependence of closed loop control operating conditions: ϕ=0.55, T_{in}=350°C, V=5.25m/sec, 100%PM, injection through four gaseous injectors(0.061" ID tubing)

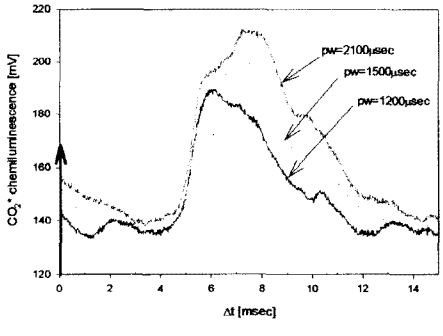

Figure 6. Response of a stable flame to pulse fuel injection
$f_{inj.}$=90Hz, natural gas injection

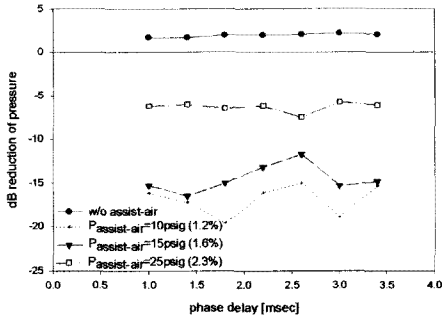

Figure 7. Closed loop control result using jet-A injection (injection frequency: fourth subharmonic, pulse width: 300μsec, addition of 8.6 % heat release by secondary fuel)

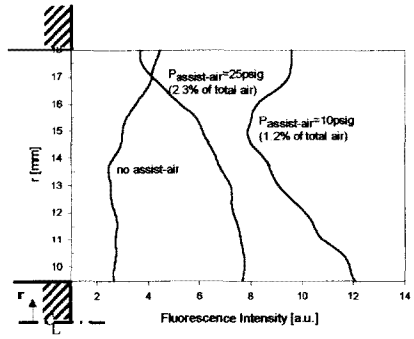

Figure 9. Fuel distribution measurement across annular passage near dump plane using PLIF of jet-A 9 milliseconds after the valve opening trigger (V=5.25m/sec, T_{in}=350°C, excitation by 266nm)

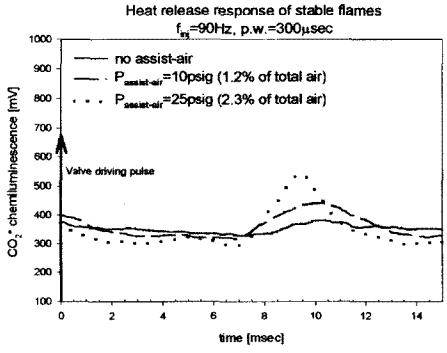

Figure 8. Heat release response of a stable flame to pulsed jet-A injection (injection frequency=90Hz, pulse width=300μsec)

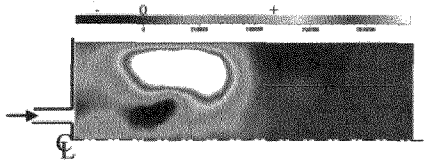

Figure 10. Rayleigh index distribution for unstable flame (100%PM, V=5.25m/sec, ϕ=0.55, T_{in}=350°C)

PAPER -35, D. Santavicca

Question (F. E. C. Culick, USA)
You discussed results for three cases of pulsed fuel injection. Are they three distinct cases or the averaged results of many tests?

Reply
The results presented are averages of many tests.

Question (C. Hassa, Germany)
If the idea of secondary fuel injection is to locally enrich the mixture, why is the position of the fuel injector so far upstream, almost as for a premixing injector?

Reply
We initially attempted to inject the secondary fuel at several locations on the dump plane. Although this was very successful when using natural gas as the secondary fuel, when using Jet-A, significant diffusion flame burning was observed. Therefore the secondary fuel injection location was moved upstream to allow sufficient time for vaporization and some degree of mixing when using liquid fuels. The specific location which was chosen, i.e., approximately 100 mm upstream of the dump lane, was selected based on previous experience with a similar configuration which showed that it was still possible to achieve significant radial stratification of the injected fuel with this injection location.

This page has been deliberately left blank

Page intentionnellement blanche